*Inorg. Chem.* **2008**, *47*, 4457−4462

# Synthesis and Characterization of Diorganohydrazido(2–) Tungsten Complexes

**Jürgen Koller, Hiral M. Ajmera, Khalil A. Abboud, Timothy J. Anderson,* and Lisa McElwee-White***

*Department of Chemistry, University of Florida, Gainesville, Florida 32611-7200, and Department of Chemical Engineering, University of Florida, Gainesville, Florida 32611-6005*

Received June 12, 2007

Diorganohydrazido(2–) complexes of tungsten $(L)Cl_4W(NNR_2)$ [$R_2$ = $Me_2$, $Ph_2$, $-(CH_2)_5-$; L = $CH_3CN$, pyridine] were synthesized by reacting the corresponding 1,1-diorganohydrazine with $WCl_6$, followed by reaction with acetonitrile or pyridine. Crystallographic structure determination of $(CH_3CN)Cl_4W(NNMe_2)$ and $(CH_3CN)Cl_4W(NNPh_2)$ allows a comparison of the structural features of the diorganohydrazido(2–) functionality with varying substituents. Mass spectrometry, thermogravimetric analysis, and preliminary chemical vapor deposition experiments were performed to determine the viability of these complexes as single-source precursors for deposition of $WN_x$ and $WN_xC_y$ films.

## Introduction

Early transition-metal complexes of diorganohydrazido(2–) ligands have appeared in the literature since the 1970s.[1–14] The potential application of these compounds as single-source precursors for the deposition of transition-metal nitrides has generated renewed interest in synthesizing them for use in materials chemistry.[15–17] One motivation for exploring the tungsten derivatives is their potential application as single-source precursors for chemical vapor deposition (CVD) or atomic layer deposition (ALD) of tungsten nitride ($WN_x$) and tungsten carbonitride ($WN_xC_y$),[18,19] materials of interest to the semiconductor industry as diffusion barriers in copper metallization schemes.[20–27] Preparing the hydrazido complexes provides an alternative to the addition of hydrazine derivatives into the carrier gas during deposition of metal nitride films, a process that has been reported to lower the deposition temperature of TiN films significantly because of the high reducing power of hydrazines toward high-valent transition metals.[28–30] In particular, it has been demonstrated

* To whom correspondence should be addressed. E-mail: lmwhite@chem.ufl.edu (L.M.-W.), tim@ufl.edu (T.J.A.). Tel.: +1-3523928768 (L.M.-W.). Fax: +1-3528460296 (L.M.-W.).

(1) Dilworth, J. R. *Coord. Chem. Rev.* **1976**, *21*, 29–62.
(2) Heaton, B. T.; Jacob, C.; Page, P. *Coord. Chem. Rev.* **1996**, *154*, 193–229.
(3) Arndtsen, B. A.; Schoch, T. K.; McElwee-White, L. *J. Am. Chem. Soc.* **1992**, *114*, 7041–7047.
(4) Crichton, B. A. L.; Dilworth, J. R.; Dahlstrom, P.; Zubieta, J. *Trans. Met. Chem.* **1980**, *5*, 316–317.
(5) DeBord, J. R. D.; George, T. A.; Chang, Y.; Chen, Q.; Zubieta, J. *Inorg. Chem.* **1993**, *32*, 785–786.
(6) Dilworth, J. R.; Richards, R. L.; Dahlstrom, P.; Hutchinson, J.; Kumar, S.; Zubieta, J. *J. Chem. Soc., Dalton Trans.* **1983**, 1489–1493.
(7) Dilworth, J. R.; Zubieta, J.; Hyde, J. R. *J. Am. Chem. Soc.* **1982**, *104*, 365–367.
(8) Glassman, T. E.; Vale, M. G.; Schrock, R. R. *J. Am. Chem. Soc.* **1992**, *114*, 8098–8109.
(9) Greco, G. E.; Schrock, R. R. *Inorg. Chem.* **2001**, *40*, 3861–3878.
(10) Green, M. L. H.; James, J. T.; Chernega, A. N. *J. Chem. Soc., Dalton Trans.* **1997**, 1719–1726.
(11) Henderson, R. A.; Oglieve, K. E. *J. Chem. Soc., Dalton Trans.* **1990**, 1093–1096.
(12) Schrock, R. R.; Glassman, T. E.; Vale, M. G.; Kol, M. *J. Am. Chem. Soc.* **1993**, *115*, 1760–1772.
(13) Sebe, E.; Heeg, M. J.; Winter, C. H. *Polyhedron* **2006**, *25*, 2109–2118.
(14) Tan, L. S.; Goeden, G. V.; Haymore, B. L. *Inorg. Chem.* **1983**, *22*, 1744–1750.
(15) Baunemann, A.; Kim, Y.; Winter, M.; Fischer, R. A. *J. Chem. Soc., Dalton Trans.* **2005**, 121–128.
(16) Banerjee, S.; Odom, A. L. *Organometallics* **2006**, *25*, 3099–3101.
(17) McElwee-White, L. *Dalton Trans.* **2006**, 5327–5333.
(18) Becker, J. S.; Suh, S.; Wang, S.; Gordon, R. G. *Chem. Mater.* **2003**, *15*, 2969–2976.
(19) Chiu, H. T.; Chuang, S. H. *J. Mater. Res.* **1993**, *8*, 1353–1360.
(20) Ivanova, A. R.; Galewski, C. J.; Sans, C. A.; Seidel, T. E.; Grunow, S.; Kumar, K.; Kaloyeros, A. E. *Mater. Res. Soc. Symp. Proc.* **1999**, *564*, 321–326.
(21) Singer, P. *Semicond. Int.* **2002**, *25*, 46–53.
(22) Shaw, M. J.; Grunow, S.; Duquette, D. J. *J. Electron. Mater.* **2001**, *30*, 1602–1608.
(23) ITRS. *International Technology Roadmap for Semiconductors: 2005 Edition*; International SEMATECH: Austin, TX, 2002.
(24) Galewski, C.; Seidel, T. *Eur. Semicond.* **1999**, 31–32.
(25) Kim, S.-H.; Oh, S. S.; Kim, H.-M.; Kang, D.-H.; Kim, K.-B.; Li, W.-M.; Haukka, S.; Tuominen, M. *J. Electrochem. Soc.* **2004**, *151*, C272–C282.
(26) Kim, S.-H.; Oh, S. S.; Kim, K.-B.; Kang, D.-H.; Li, W.-M.; Haukka, S.; Tuominen, M. *Appl. Phys. Lett.* **2003**, *82*, 4486–4488.
(27) Li, W.-M.; Tuominen, M.; Haukka, S.; Sprey, H.; Raaijmakers, I. J. *Solid State Technol.* **2003**, *46*, 103104, 106.
(28) Wierda, D. A.; Amato-Wierda, C. *Proc. Electrochem. Soc.* **2000**, *13*, 497–504.

10.1021/ic701151m CCC: $40.75 
Published on Web 09/15/2007

that diorganohydrazido(2–) titanium complexes serve as precursors for the deposition of titanium nitride films.[31] Incorporation of the diorganohydrazido(2–) functionality into the metal coordination sphere resulted in viable single-source precursors for the deposition of TiN thin films while maintaining the positive effects of hydrazine as a coreactant.[32]

Previously, we reported that the tungsten imido complexes $(RCN)Cl_4W(N^iPr)$, $(RCN)Cl_4W(NPh)$, and $(RCN)Cl_4W(NC_3H_5)$ (R = Me, Ph) could be used as single-source precursors for $WN_x$ and $WN_xC_y$ deposition.[33–36] Recently reported uses of 1,1-dialkylhydrazido(2–) complexes in the CVD of other materials suggested that the $(RCN)Cl_4W(NNR_2)$ derivatives of our imido complexes could be effective precursors for the CVD/ALD of $WN_x$ and $WN_xC_y$. Herein, we describe the synthesis and characterization of a series of diorganohydrazido(2–) tungsten complexes and briefly discuss their application in the CVD of $WN_xC_y$.

## Experimental Procedures

**General Procedures.** Unless specified otherwise, all manipulations were performed under an inert atmosphere ($N_2$) using standard Schlenk or glovebox techniques. All reaction solvents were purified using an MBraun MB-SP solvent purification system prior to use. NMR solvents were degassed by three freeze−pump−thaw cycles and stored over 4 Å molecular sieves in an inert-atmosphere glovebox. $^1$H and $^{13}$C NMR spectra were recorded on Gemini 300, Mercury 300, or VXR 300 spectrometers using residual protons of deuterated solvents for reference. Pentane, pyridine, acetonitrile, and benzonitrile (all anhydrous) were used as received from Aldrich. 1,1-Dimethylhydrazine, 1,1-diphenylhydrazine, and 1-aminopiperidine were degassed by three freeze−pump−thaw cycles and stored over 4 Å molecular sieves. All other chemicals were used as received without further purification. Thermogravimetric analysis (TGA) was carried out using a Perkin-Elmer TGA7 thermogravimetric analyzer under nitrogen with a heating rate of 10 °C/min (sample size ≈ 3 mg). $^1$H NMR spectra for kinetic studies were recorded on a Varian Inova spectrometer at a frequency of 500 MHz, on a 5 mm indirect detection probe. The variable-temperature spectra were recorded on automation. To achieve temperature stability, for each temperature step of 2 °C, a preacquisition delay of 1200 s was followed by shimming on the lock level. The spectra were collected in 64 transients, with an acquisition time of 5 s. No relaxation delay and no apodization were used. The simulation of the spectra was done using the *gNMR* program.[37] All mass spectral analyses were performed using a Thermo Trace DSQ (quadrupole MS) mass spectrometer with a heated probe (Thermo Finnigan, San Jose, CA).

Crystallinity of films deposited by CVD was examined by X-ray diffraction (XRD) using a Phillips APD 3720 system. Cu Kα radiation generated at 40 kV and 20 mA was used for the XRD analysis. Film composition and atomic bonding were obtained from X-ray photoelectron spectroscopy (XPS) measurements. The XPS spectra were taken using monochromatic Mg Kα radiation, with the X-ray source operating at 300 W (15 kV and 20 mA). The film thickness was measured by cross-sectional scanning electron microscopy (SEM) on a JEOL JSM-6335F.

**$(CH_3CN)Cl_4W(NNMe_2)$ (1).** A Schlenk flask was charged with $WCl_6$ (2.10 g, 5.30 mmol) and 40 mL of methylene chloride. 1,1-Dimethylhydrazine (0.39 mL, 5.2 mmol) was added via syringe under vigorous stirring at −78 °C. After 10 min of stirring, the solvent was removed in vacuo during warming to room temperature. Acetonitrile (15 mL) was added via syringe, and the mixture was stirred for an additional 30 min. The solvent was removed in vacuo and the solid extracted with 2 × 15 mL of methylene chloride. The combined extracts were filtered, and the volume was reduced to 15 mL. The product was precipitated by adding the solution into vigorously stirred pentane (200 mL) at 0 °C. The orange product was filtered off as a microcrystalline powder and dried in vacuo. Yield: 1.66 g (75%, 3.92 mmol). $^1$H NMR (benzene-$d_6$, 25 °C): δ 5.35 (s, 6H, $N(CH_3)_2$), 0.15 (s, 3H, $CH_3CN$). $^{13}$C NMR (benzene-$d_6$, 25 °C): δ 0.58 ($CH_3CN$), 36.89 ($N(CH_3)_2$), 120.86 ($CH_3CN$). Anal. Calcd for $C_4H_9Cl_4N_3W$: C, 11.31; H, 2.14; N, 9.89. Found: C, 10.89; H, 1.97; N, 9.52.

**$(CH_3CN)Cl_4W(Npip)$ (2).** A Schlenk flask was charged with $WCl_6$ (2.00 g, 5.04 mmol) and 40 mL of methylene chloride. 1-Aminopiperidine (0.53 mL, 4.9 mmol) was added via syringe under vigorous stirring at −78 °C. After 10 min of stirring, the solvent was removed in vacuo during warming to room temperature. Acetonitrile (15 mL) was added via syringe, and the mixture was stirred for an additional 30 min. The solvent was removed in vacuo and the solid extracted with 2 × 20 mL of methylene chloride. The extract was filtered and the volume reduced to 15 mL. The product was precipitated by adding the methylene chloride solution into vigorously stirred pentane (200 mL) at 0 °C. The rust-colored product was filtered off as a microcrystalline powder and dried in vacuo. Yield: 1.75 g (76%, 3.76 mmol). $^1$H NMR (benzene-$d_6$, 25 °C): δ 4.86 (t, 4H, $NCH_2$), 1.34 (m, 4H, $CH_2$), 1.01 (m, 2H, $CH_2$), 0.17 (s, 3H, $CH_3CN$). $^{13}$C NMR (benzene-$d_6$, 25 °C): δ 0.75 ($CH_3CN$), 22.73 ($CH_2$), 30.70 ($CH_2$), 51.00 ($NCH_2$), 120.78 ($CH_3CN$).

**$(CH_3CN)Cl_4W(NNPh_2)$ (3).** A Schlenk flask was charged with $WCl_6$ (2.00 g, 5.04 mmol) and 40 mL of methylene chloride. 1,1-Diphenylhydrazine (0.91 g, 4.9 mmol) was added via syringe under vigorous stirring at −78 °C. After 10 min of stirring, the solvent was removed in vacuo during warming to room temperature. Acetonitrile (15 mL) was added via syringe, and the mixture was stirred for an additional 30 min. The solvent was removed in vacuo and the solid extracted with 2 × 20 mL of methylene chloride. The combined extracts were filtered, and the volume was reduced to 15 mL. The product was precipitated by adding the solution into vigorously stirred pentane (200 mL) at 0 °C. The deep-purple product was filtered off as a microcrystalline powder and dried in vacuo. Yield: 2.07 g (76%, 3.77 mmol). $^1$H NMR (benzene-$d_6$, 25 °C): δ 7.15 (br s, 8H, Ph), 6.53–6.47 (m, 2H, Ph), 0.11 (s, 3H, $CH_3CN$). $^{13}$C NMR (benzene-$d_6$, 25 °C): δ 0.97 ($CH_3CN$), 121.23 ($CH_3CN$), 125.65 (Ph), 125.77 (Ph), 128.80 (Ph), 128.94 (Ph),

(29) Amato-Wierda, C.; Wierda, D. A. *J. Mater. Res.* **2000**, *15*, 2414–2424.
(30) Amato-Wierda, C.; Norton, E. T.; Wierda, D. A., Jr. *Mater. Res. Soc. Symp. Proc.* **2000**, *606*, 91–96.
(31) Winter, C. H.; McKarns, P. J.; Scheper, J. T. *Mater. Res. Soc. Symp. Proc.* **1998**, *495*, 95–106.
(32) Scheper, J. T.; McKarns, P. J.; Lewkebandara, T. S.; Winter, C. H. *Mater. Sci. Semicond. Process.* **1999**, *2*, 149–157.
(33) Bchir, O. J.; Johnston, S. W.; Cuadra, A. C.; Anderson, T. J.; Ortiz, C. G.; Brooks, B. C.; Powell, D. H.; McElwee-White, L. *J. Cryst. Growth* **2003**, *249*, 262–274.
(34) Bchir, O. J.; Green, K. M.; Hlad, M. S.; Anderson, T. J.; Brooks, B. C.; Wilder, C. B.; Powell, D. H.; McElwee-White, L. *J. Organomet. Chem.* **2003**, *684*, 338–350.
(35) Bchir, O. J.; Kim, K. C.; Anderson, T. J.; Craciun, V.; Brooks, B. C.; McElwee-White, L. *J. Electrochem. Soc.* **2004**, *151*, G697–G703.
(36) Bchir, O. J.; Green, K. M.; Ajmera, H. M.; Zapp, E. A.; Anderson, T. J.; Brooks, B. C.; Reitfort, L. L.; Powell, D. H.; Abboud, K. A.; McElwee-White, L. *J. Am. Chem. Soc.* **2005**, *127*, 7825–7833.
(37) *gNMR*; Adept Scientific PLC: Herts, U.K., 1995.

**Scheme 1.** Synthesis of Diorganohydrazido(2–) Complexes

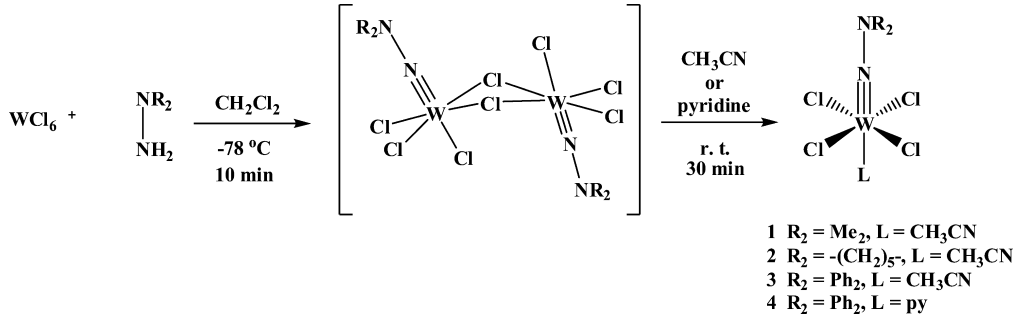


**1** $R_2 = Me_2$, L = $CH_3CN$
**2** $R_2 = -(CH_2)_5-$, L = $CH_3CN$
**3** $R_2 = Ph_2$, L = $CH_3CN$
**4** $R_2 = Ph_2$, L = py

130.53 (Ph), 130.65 (Ph), 131.39 (Ph), 131.61 (Ph), 133.38 ($C_{ipso}$), 135.34 ($C_{ipso}$).

**(py)$Cl_4$W(NNPh$_2$) (4).** A Schlenk flask was charged with $WCl_6$ (2.00 g, 5.04 mmol) and 40 mL of methylene chloride. 1,1-Diphenylhydrazine (0.91 g, 4.94 mmol) was added via syringe under vigorous stirring at −78 °C. After 10 min of stirring, the solvent was removed in vacuo during warming to room temperature. Pyridine (15 mL) was added via syringe, and the mixture was stirred for an additional 30 min. The solvent was removed in vacuo and the solid extracted with 2 × 30 mL of benzene. The combined extracts were filtered, and the solvent was removed in vacuo to afford **4** in 27% yield as a dark-red microcrystalline solid (0.81 g, 1.38 mmol). $^1$H NMR (benzene-$d_6$, 25 °C): $\delta$ 9.58–9.55 (m, 2H), 7.19–7.11 (m, 10H), 6.68–6.36 (m, 3H). $^{13}$C NMR (benzene-$d_6$, 25 °C): $\delta$ 118.56, 121.51, 124.02, 124.73, 125.98, 128.86, 128.91, 129.89, 130.67, 133.46, 139.32, 143.95, 152.91. Anal. Calcd for $C_{17}H_{15}Cl_4N_3W$: C, 34.79; H, 2.58; N, 7.16. Found: C, 34.60; H, 2.31; N, 6.96.

**Crystallographic Structure Determination of 1 and 3.** Data were collected at 173 K on a Siemens SMART PLATFORM equipped with a CCD area detector and a graphite monochromator utilizing Mo Kα radiation ($\lambda$ = 0.710 73 Å). Cell parameters were refined using up to 8192 reflections. A full sphere of data (1850 frames) was collected using the $\omega$-scan method (0.3° frame width). The first 50 frames were remeasured at the end of data collection to monitor instrument and crystal stability (the maximum correction on $I$ was <1%). Absorption corrections by integration were applied based on measured indexed crystal faces.

The structure was solved by the direct methods in *SHELXTL6*[38] and refined using full-matrix least squares. The non-H atoms were treated anisotropically, whereas the H atoms were calculated in ideal positions and were riding on their respective C atoms. For compound **1**, the molecules are located on 2-fold rotation axes. A total of 60 parameters were refined in the final cycle of refinement using 1228 reflections with $I > 2\sigma(I)$ to yield R1 and wR2 of 3.25% and 7.93%, respectively. For compound **3**, the highest electron density peak in the final difference Fourier map is most likely the result of a small disorder in one of the phenyl rings. The disorder could not be resolved. A total of 399 parameters were refined in the final cycle of refinement using 6166 reflections with $I > 2\sigma(I)$ to yield R1 and wR2 of 2.74% and 5.84%, respectively. Refinement was done using $F^2$.

## Results and Discussion

The tungsten hydrazido complexes **1**–**4** were prepared by reacting the corresponding diorganohydrazine with $WCl_6$ in methylene chloride at −78 °C (Scheme 1). The resulting Cl-bridged tungsten dimer was not isolated but was subsequently treated with acetonitrile or pyridine to yield compounds **1**–**4** as orange, rust-colored, purple, and red solids, respectively. $^1$H and $^{13}$C NMR spectra are in good agreement with the symmetry equivalence of the substituents on the hydrazido functionality in compounds **1** and **2**. Contrary to this finding, NMR spectra reveal the inequivalence of the two phenyl rings in compounds **3** and **4**.

Single crystals suitable for XRD were obtained from compounds **1** and **3**, and their structures were determined. Crystal data and structure refinement for these complexes can be found in Table 1. Compound **1** adopts a pseudooctahedral geometry as shown in the ORTEP representation of **1** (Figure 1). The W−Cl bond distances are on the order of 2.34 Å,[39] which is within the expected range for $W^{VI}$−Cl bonds. The short W−N1 bond distance [1.769(5) Å] and a short bond distance of 1.271(8) Å between N1 and N2 suggest a high degree of delocalization and significant multiple-bond character throughout the W1−N1−N2 unit, which is consistent with other hydrazido complexes of tungsten with multiple chloride ligands such as [W($\eta^5$-$C_5Me_5$)$Cl_3$(NNPh$_2$)][40] [W−N 1.769(2) Å; N−N 1.296(3) Å] and *cis*-[$WCl_3$(NNH$_2$)(PMe$_2$Ph)$_2$][41] [W−N 1.752(10) Å; N−N 1.300(17) Å]. This observation can be explained based upon two possible limiting electronic structures, **A** and **B**, with representation **A** being the major contributor. Furthermore, the

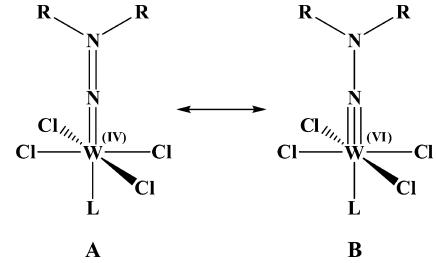


**A** **B**

W1−N3 bond distance of 2.224(7) Å is significantly shorter than those reported for related tungsten imido compounds,[36] suggesting a decreased trans influence of the diorganohydrazido(2–) ligand compared to the imido moiety. A list of selected bond lengths and angles for **1** is given in Table 2.

(38) *SHELXTL6*; Bruker AXS: Madison, WI, 2000.

(39) Orpen, A. G.; Brammer, L.; Allen, F. H.; Kennard, O.; Watson, D. G.; Taylor, R. *J. Chem. Soc., Dalton Trans.* **1989**, S1–S83.
(40) Redshaw, C.; Gibson, V. C.; Clegg, W.; Edwards, A. J.; Miles, B. *J. Chem. Soc., Dalton Trans.* **1997**, 3343–3347.
(41) Chatt, J.; Fakley, M. E.; Hitchcock, P. B.; Richards, R. L.; Luong-Thi, N. T. *J. Chem. Soc., Dalton Trans.* **1982**, 345–352.

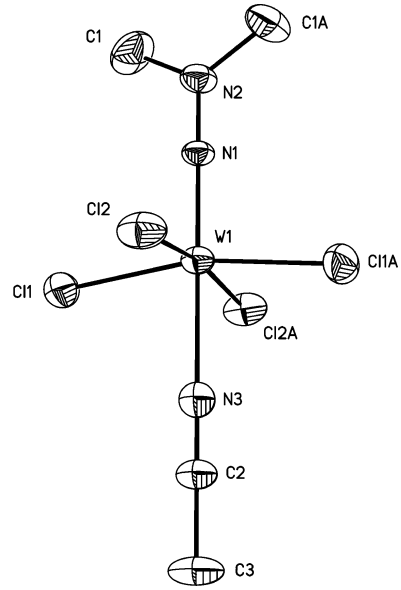


**Figure 1.** Thermal ellipsoids diagram of the molecular structure of **1**. Thermal ellipsoids are drawn at 50% probability. H atoms are omitted for clarity.

**Table 1.** Crystal Data and Structure Refinement for Complexes **1** and **3**

| | **1** | **3** |
|---|---|---|
| complex | | |
| empirical formula | $C_4H_9Cl_4N_3W$ | $C_{28}H_{26}Cl_8N_6W_2$ |
| fw | 424.79 | 1097.85 |
| $T$ (K) | 173(2) | 173(2) |
| wavelength (Å) | 0.710 73 | 0.710 73 |
| cryst syst | monoclinic | monoclinic |
| space group | $C2/c$ | $P2_1/n$ |
| unit cell dimens | | |
| $a$ (Å) | 8.7700(7) | 10.8288(8) |
| $b$ (Å) | 13.8203(11) | 17.8753(13) |
| $c$ (Å) | 9.7343(8) | 18.2409(13) |
| α (deg) | 90 | 90 |
| $\beta$ (deg) | 100.575(2) | 101.006(1) |
| $\gamma$ (deg) | 90 | 90 |
| $V$ (Å$^3$) | 1159.80(16) | 3465.9(4) |
| $Z$ | 4 | 4 |
| density (Mg/m$^3$) | 2.433 | 2.104 |
| abs coeff (mm$^{-1}$) | 10.837 | 7.280 |
| $F$(000) | 784 | 2080 |
| cryst size (mm$^3$) | 0.19 × 0.15 × 0.08 | 0.12 × 0.11 × 0.04 |
| $\theta$ range for data collection (deg) | 2.78–27.49 | 1.61–27.50 |
| index ranges | $-8 \le h \le 11$<br>$-17 \le k \le 15$<br>$-12 \le l \le 11$ | $-14 \le h \le 13$<br>$-22 \le k \le 23$<br>$-21 \le l \le 23$ |
| reflns colld | 3683 | 23 178 |
| indep reflns ($R_{int}$) | 1333 (0.1092) | 7931 (0.0559) |
| completeness to $\theta = 24.60$ (%) | 99.4 | 99.7 |
| abs corrn | integration | integration |
| max and min transmn | 0.5020 and 0.1814 | 0.7594 and 0.4754 |
| data/restraints/param | 1333/0/60 | 7931/0/399 |
| GOF on $F^2$ | 1.027 | 0.961 |
| R1[a] | 0.0325 | 0.0274 |
| wR2[b] | 0.0793 | 0.0584 |
| largest diff peak and hole/e·Å$^3$ | +4.084 and −1.814 | 1.264 and −0.947 |

[a] $R1 = \sum(||F_o| - |F_c||)/\sum|F_o|$. [b] $wR2 = [\sum[w(F_o^2 - F_c^2)^2]/\sum[w(F_o^2)^2]]^{1/2}$. $S = [\sum[w(F_o^2 - F_c^2)^2](n - p)]^{1/2}$, $w = 1/[\sigma^2(F_o^2) + (mp)^2 + np]$, $p = [\max(F_o^2,0) + 2F_c^2]/3$.

The structure of compound **3** shows similarities to that of compound **1**. Complex **3** also exhibits a pseudooctahedral geometry at the tungsten center (Figure 2). However, the W1−N1 bond distance of 1.742(4) Å and the N1−N2 distance of 1.312(5) Å suggest less conjugation throughout the hydrazido moiety as compared to compound **1**. One hydrazido phenyl ring is coplanar with the N2−N1−W1 unit, maximizing the conjugation between the two subunits, as has been observed for other 1,1-diphenylhydrazido complexes of tungsten.[42] This additional mode of conjugation decreases the electron density between N1 and N2, resulting in a noteworthy elongation of the N−N bond. In addition, the slightly shorter W−N bond suggests higher $\pi$-bonding character such that compound **3** may be better described by representation **B**. The large bond angles of N1−W1−Cl2 and N1−W1−Cl3 of 99.2° and 98.0°, respectively, reflect

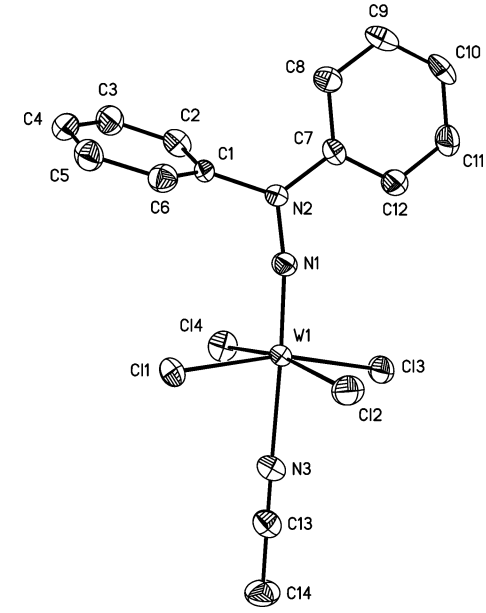


**Figure 2.** Thermal ellipsoids diagram of the molecular structure of **3**. Thermal ellipsoids are drawn at 50% probability. H atoms are omitted for clarity.

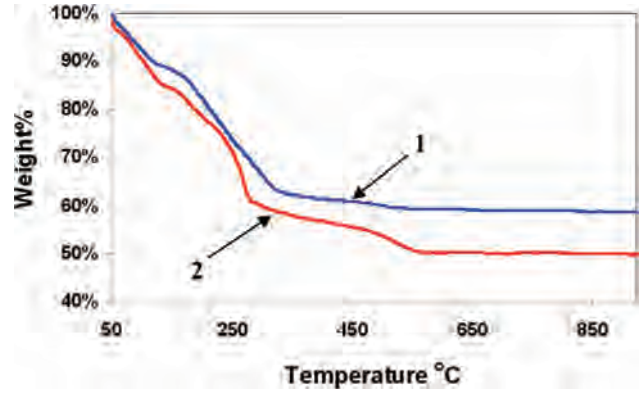


**Figure 3.** TGA curve of compounds **1** and **2** recorded at a heating rate of 10 °C/min under nitrogen.

**Table 2.** Selected Bond Distances (Å) and Angles (deg) for Compound **1**

| | | | | | |
|---|---|---|---|---|---|
| W1−N1 | 1.769(5) | N1−W1−N3 | 180.000(1) | N2−N1−W1 | 180.0(0) |
| W1−N3 | 2.224(7) | N1−W1−Cl1 | 96.85(4) | N1−N2−C1 | 119.1(4) |
| W1−Cl1 | 2.3374(16) | N3−W1−Cl1 | 83.15(4) | C1−N2−C1A | 121.9(7) |
| W1−Cl2 | 2.3562(16) | N1−W1−Cl2 | 95.02(3) | | |
| N1−N2 | 1.271(8) | N3−W1−Cl2 | 84.98(3) | | |
| N2−C1 | 1.438(7) | Cl1−W1−Cl2 | 89.25(7) | | |

(42) Niemoth-Anderson, J. D.; Debord, J. R. D.; George, T. A.; Ross, C. R., II; Stezowski, J. J. *Polyhedron* **1996**, *15*, 4031–4040.

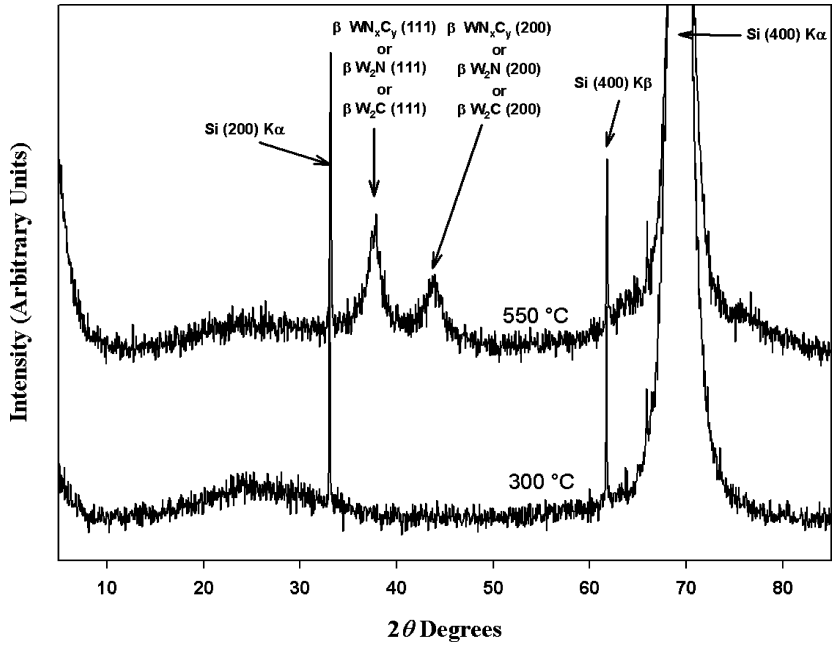


**Figure 4.** XRD patterns for films deposited at 300 and 550 °C from **1** on a Si(100) substrate.

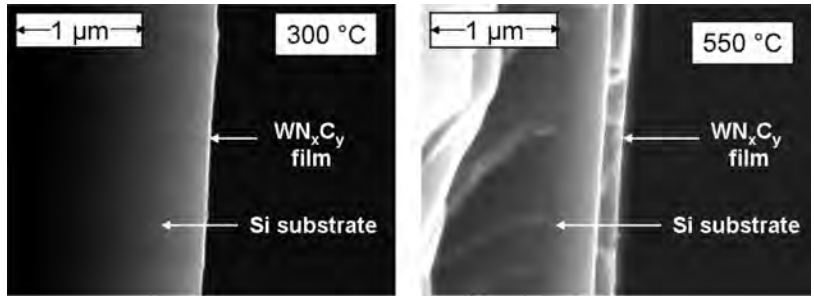


**Figure 5.** SEM images for films deposited at 300 and 550 °C from **1** on a Si(100) substrate.

**Table 3.** Selected Bond Distances (Å) and Angles (deg) for Compound **3**

| | | | | | |
|---|---|---|---|---|---|
| N1−N1 | 1.742(4) | N1−N2 | 1.312(5) | N1−N1−Cl4 | 91.80(11) |
| N1−N3 | 2.216(4) | N2−C1 | 1.447(5) | N3−N1−N1 | 174.91(14) |
| N1−Cl1 | 2.3191(11) | N2−C7 | 1.429(6) | N1−N1−N2 | 169.8(3) |
| N1−Cl2 | 2.3445(11) | N1−N1−Cl1 | 96.58(11) | N1−N2−C1 | 115.0(4) |
| N1−Cl3 | 2.3519(11) | N1−N1−Cl2 | 99.15(11) | N1−N2−C7 | 120.7(3) |
| N1−Cl4 | 2.3537(11) | N1−N1−Cl3 | 98.02(11) | C1–N2−C7 | 123.6(4) |

the increased steric demand of the coplanar phenyl ring. A list of selected bond lengths and angles for **3** is given in Table 3.

The thermal behavior of compounds **1** and **2** was investigated as preliminary screening for use of complexes **1**–**4** as precursors for the metal−organic CVD of $WN_x$. TGA experiments were run at a heating rate of 10 °C/min from 50 to 900 °C. The TGA curves of **1** and **2** show residual masses of 58 and 50%, respectively, which are constant above 550 °C (Figure 3). In both cases, an initial drop in mass of about 10% is observed corresponding to the loss of the acetonitrile ligand. Because this dissociation is observed in the low-temperature range, it can be assumed that the acetonitrile is bound weakly to the tungsten metal center.

To corroborate this observation, the kinetics of acetonitrile exchange were determined via NMR spectroscopy. The sample for the exchange study was prepared in the glovebox by dissolving complex **1** and an approximately equivalent amount of acetonitrile in toluene-$d_8$. The $^1$H NMR spectrum of this sample at 40 °C displayed the signals for **1** at 0.53 ppm and acetonitrile at 0.83 ppm, in a ratio of 1:2.09. The exchange of **1** with acetonitrile was monitored by $^1$H NMR in a temperature range from 40 to 84 °C. The exchange rate $k$ was determined by line-shape analysis in the temperature interval 50–84 °C. A plot of $\ln(k/T)$ vs $1/T$ in the temperature interval from 50 to 84 °C afforded an activation enthalpy of 23.0 kcal/mol and an activation entropy of 28.8 cal/mol·K, consistent with dissociative exchange. The corresponding Gibbs free energy of activation is 14.4 kcal/mol.

Because a correlation between the mass spectrometric fragmentation patterns of precursors and likely decomposition pathways during CVD has been postulated in the literature,[36,43,44] mass spectra were obtained from compounds **1**–**3**. Table 4 summarizes the major fragment ions observed in the positive-ion chemical ionization (CI) spectra of compounds **1**–**3**. No molecular ion peak was observed in the CI spectrum of **1**, **2**, or **3**, consistent with facile loss of the acetonitrile ligand. Instead, the highest values were in mass envelopes at $m/z$ 384, 354, and 508, corresponding to

(43) Lewkebandara, T. S.; Sheridan, P. H.; Heeg, M. J.; Rheingold, A. L.; Winter, C. H. *Inorg. Chem.* **1994**, *33*, 5879–5889.
(44) Amato, C. C.; Hudson, J. B.; Interrante, L. V. *Mater. Res. Soc. Symp. Proc.* **1990**, *168*, 119–124.

**Table 4.** Summary of Relative Abundances for Positive-Ion CI Mass Spectra of Compounds **1**–**3**

| compound | CI fragment | *m*/*z* | abundance[a] |
|---|---|---|---|
| **1** | $[Cl_4W(NNMe_2)]^+$ | 384 | 8 |
| | $[Cl_3W(NNMe_2)]^+$ | 349 | 100 |
| | $[Cl_3W]^+$ | 289 | 4 |
| **2** | $[Cl_2W(HN\text{-}pip)]^+$ | 354 | 30 |
| | $[Cl_3W]^+$ | 289 | 12 |
| | $[Me_2pip]^+$ | 114 | 18 |
| | $[H_2pip]^+$ | 86 | 70 |
| | $[pip]^+$ | 84 | 100 |
| **3** | $[Cl_4W(NNPh_2)]^+$ | 508 | 5 |
| | $[Cl_3W(NNPh_2)H]^+$ | 473 | 21 |
| | $[Cl_3WNH_2]^+$ | 307 | 4 |
| | $[Ph_2NMe_2]^+$ | 198 | 19 |
| | $[Ph_2NH_2]^+$ | 170 | 100 |

[a] Relative abundances were adjusted by summing the observed intensities for the predicted peaks of each mass envelope and normalizing the largest sum to 100%.

$[Cl_4W(NNMe_2)]^+$, $[Cl_2W(HN\text{-}pip)]^+$, and $[Cl_4W(NNPh_2)]^+$, respectively. The base peak in the CI spectrum of **1** was observed at *m*/*z* 349, corresponding to the $[Cl_3W(NNMe_2)]^+$ fragment. Interestingly, the base peaks in the CI spectra of **2** and **3** at *m*/*z* 84 and 170, corresponding to the $[pip]^+$ and $[Ph_2NH_2]^+$ fragments, respectively, are indicative of the hydrazido N−N bond being broken under ionization conditions, which is additionally supported by the presence of the $[Cl_3WNH_2]^+$ fragment in the CI spectrum of **3** at *m*/*z* 307. Cleavage of the N−N bond would also be on the pathway for decomposition of **2** and **3** to $WN_x$ films under CVD conditions.

Preliminary CVD experiments were performed in the temperature range of 300–700 °C in 50 °C increments. A custom cold-wall CVD reactor was used in these screening experiments and has been discussed elsewhere.[34] The lowest temperature for film deposition from **1** was 300 °C. The color of the deposited film varied from golden brown at low deposition temperature to grayish at higher deposition temperature. Figure 4 shows the XRD spectra for films deposited from **1** at 300 and 550 °C. The XRD measurement for deposition at 300 °C shows peaks assignable to only the silicon substrate, indicating that the film is X-ray amorphous. Crystallinity first appears for the film deposited at 550 °C, as indicated by the two peaks at $2\theta = 37.65$ and 43.50° in the XRD pattern for this sample. The peak position indicates the presence of $\beta$-$W_2N$, $\beta$-$W_2C$, or their solid solution $\beta$-$WN_xC_y$ phase. Because the XRD peak position for both the (111) and (200) reflections of $\beta$-$W_2N$ and $\beta$-$W_2C$ is within $2\theta = 0.95°$, accurate phase identification was not possible from XRD measurement. Thus, XPS measurements were taken to obtain the bonding state of different atoms in the film. XPS spectra (not shown) revealed that both N and C atoms are bonded to W. From XRD and XPS measurements, it can be concluded that the film deposited from **1** consists of either a mixture of $\beta$-$W_2N$ and $\beta$-$W_2C$ phases or single-phase $\beta$-$WN_xC_y$. Film composition measurement by XPS showed that the film contained W, N, C, and O atoms. No Cl atom impurity was present within the detection limits of XPS (ca. 1 atom %). Figure 5 shows cross-sectional images obtained from SEM for films deposited at 300 and 550 °C. The film growth rate for deposition at 300 and 550 °C was 1.3 and 10.4 Å/min, respectively. A detailed report on the characterization and diffusion barrier performance of films from **1**–**3** is forthcoming.

## Conclusions

In conclusion, we have prepared the diorganohydrazido-(2–) tungsten complexes $(L)Cl_4W(NNR_2)$ [**1**–**4**; $R_2 = Me_2$, $Ph_2$, $-(CH_2)_5-$; L = $CH_3CN$, pyridine] by reacting the corresponding 1,1-diorganohydrazines with tungsten hexachloride followed by treatment with acetonitrile or pyridine. The crystallographic structure determination of $(CH_3CN)Cl_4W(NNMe_2)$ and $(CH_3CN)Cl_4W(NNPh_2)$ allows a comparison of the structural features of the diorganohydrazido functionality as the hydrazido substituents R are varied. Preliminary experiments suggest that compound **1** is a viable single-source precursor for the deposition of $WN_xC_y$ films. Further CVD experiments and subsequent film characterization are underway.

**Acknowledgment.** We thank the National Science Foundation for support under NSF-CRC Grant CHE-0304810. K.A.A. acknowledges the National Science Foundation and the University of Florida for funding of the purchase of the X-ray equipment. Giovanni Rojas provided assistance with the TGA measurements.

**Supporting Information Available:** $^1H$ NMR spectra of complexes **1**–**3** and tables of bond distances, bond angles, positional parameters, and anisotropic displacement parameters for **1** and **3**. This material is available free of charge via the Internet at http://pubs.acs.org.

IC701151M